



# <sup>18</sup>F-FDOPA-PET in pseudotumoral brain lesions

Dimitri Renard<sup>1</sup> · Laurent Collombier<sup>2</sup> · Sabine Laurent-Chabalier<sup>3</sup> · Thibault Mura<sup>3</sup> · Anne Le Floch<sup>1</sup> · Hassan El Fertit<sup>4</sup> · Eric Thouvenot<sup>1,5</sup> · Jean Sebastien Guillamo<sup>1</sup>

Received: 29 June 2020 / Revised: 8 October 2020 / Accepted: 10 October 2020 / Published online: 21 October 2020  
© Springer-Verlag GmbH Germany, part of Springer Nature 2020

## Abstract

**Introduction** 3,4-Dihydroxy-6-[<sup>18</sup>F]-fluoro-L-phenylalanine (FDOPA) positron emission tomography (PET) is sensitive for identifying primary brain tumors. However, increased FDOPA uptake has been reported in pseudotumoral brain lesions. Our aim was to analyse FDOPA-PET in patients with pseudotumoral brain lesions and to compare them with patients with brain tumors.

**Methods** We retrospectively analysed consecutively recruited patients with suspected primary brain tumor (based on clinical and magnetic resonance imaging findings) referred for FDOPA-PET in our centre between November 2013 and June 2019 ( $n = 74$ ). FDOPA-PET parameters (maximum and mean lesion standardised uptake values [SUV] and ratios comparing lesion with different background uptake SUV) and thresholds were evaluated to determine which offered optimal discrimination between pseudotumoral and tumoral lesions.

**Results** Overlapping PET values were observed between pseudotumoral ( $n = 26$ ) and tumoral ( $n = 48$ ) lesion, particularly for low-grade tumors. Based on receiver operating characteristic (ROC) analyses, the optimal PET parameters to discriminate pseudotumoral from tumoral lesions were  $SUV_{max}$  lesion/basal ganglia,  $SUV_{max}$  lesion/grey matter,  $SUV_{mean}$  lesion/grey matter, and  $SUV_{max}$  lesion/mirror area in contralateral hemisphere (all ratios showing area under the curve [AUC] 0.85, 95% CI). The narrowest 95% sensitivity–95% specificity window was observed for  $SUV_{max}$  lesion/basal ganglia ratio, with ratio values of 0.79 and 1.35 corresponding to 95% sensitivity and 95% specificity, respectively.

**Conclusion** FDOPA-PET uptake should be interpreted with caution in patients with suspected primary brain tumor, especially in patients showing low or intermediate SUV values and ratios.

**Clinical Trial Registration-URL** <https://www.clinicaltrials.gov>. Unique identifier: NCT04306484

**Keywords** Tumor · Pseudotumor · 3,4-dihydroxy-6-[<sup>18</sup>F]-fluoro-L-phenylalanine · FDOPA · PET

**Electronic supplementary material** The online version of this article (<https://doi.org/10.1007/s00415-020-10269-9>) contains supplementary material, which is available to authorized users.

✉ Dimitri Renard  
dimitrirenard@hotmail.com

<sup>1</sup> Department of Neurology, CHU Nîmes, University Montpellier, Nîmes, France

<sup>2</sup> Department of Nuclear Medicine, CHU Nîmes, University Montpellier, Nîmes, France

<sup>3</sup> Department of Biostatistics, Clinical Epidemiology, Public Health, and Innovation in Methodology, CHU Nîmes, University Montpellier, Nîmes, France

<sup>4</sup> Department of Neurosurgery, CHU Nîmes, University Montpellier, Nîmes, France

<sup>5</sup> Institut de Génomique Fonctionnelle, UMR5203, INSERM 1191, University Montpellier, Montpellier, France

## Introduction

Amino acid tracers present several advantages over <sup>18</sup>F-2-fluoro-2-deoxy-D-glucose for positron emission tomography (PET) imaging of brain tumors (especially in low-grade tumors due to the lower background uptake of amino acid tracers compared with <sup>18</sup>F-2-fluoro-2-deoxy-D-glucose). They are now considered as the tracers of choice for initial and progression diagnosis and for evaluation of treatment response [1]. Amino acid PET tracers include <sup>11</sup>C-methyl-L-methionine (MET), *O*-(2-[<sup>18</sup>F]fluoroethyl)-L-tyrosine (FET), and 3,4-dihydroxy-6-[<sup>18</sup>F]-fluoro-L-phenylalanine (FDOPA). The uptake of radiolabelled amino acids is based on the expression of the Na<sup>+</sup>-independent large neutral amino acid transporters (LAT1 and LAT2) on the cell surface of tumor cells, which are relatively independent from

blood–brain barrier permeability allowing these tracers to depict non contrast-enhancing brain tumor regions [2]. MET and FDOPA uptake is thought to be largely due to LAT1, while FET is transported by both LAT1 and LAT2. No relevant differences have been shown between available radiolabelled amino acids in terms of tumor to brain contrast, although differences exist concerning tracer biodistribution in the brain and the time-activity curves of tracer uptake [3–5]. In general, higher uptake is observed in patients with a high-grade tumor compared with those with a low-grade tumor, with the exception of oligodendroglioma which sometimes show higher uptake than high-grade astrocytomas, likely due to their increased cellular and vascular density in this glioma subtype [6–12]. FDOPA is a substrate for the enzyme aromatic amino acid decarboxylase in dopaminergic neurons, explaining the prominent physiological uptake by the basal ganglia (BG). Although amino acid PET shows high accuracy for the detection of brain tumors, increased uptake has been reported in numerous pseudotumoral brain lesions (including inflammatory, infectious, vascular, seizure-related, and brain developmental lesions) [8, 9, 13–22].

The largest amino acid PET study analysing pseudotumoral lesions used FET tracer. In that retrospective study of a large unselected patient population ( $n = 393$ ), one-third of the 87 patients with a pseudotumoral lesion showed increased uptake reflecting the low specificity of 68% (but relatively high sensitivity of 87%) for brain tumor diagnosis, with uptake values in pseudotumoral lesions in the same range as low-grade brain tumors [9].

For FDOPA-PET, only case reports and small series of pseudotumoral lesions showing increased uptake have been reported [14–16, 19–22].

In studies reporting on amino acid PET in pseudotumoral and tumoral lesions, different PET parameters and standardised uptake value (SUV) cut-offs were used to determine the presence of increased uptake and so-called PET positivity. A minority of studies assessed optimal discriminating SUV thresholds (i.e. optimal combined sensitivity and specificity, or analyses favouring higher sensitivity or specificity).

Our aims were to compare FDOPA-PET performed in patients with pseudotumoral and (low- and high-grade) tumoral brain lesions, and to determine optimal PET parameters and thresholds to discriminate both lesion types.

## Methods

### Patient population

We retrospectively analysed consecutive patients referred for FDOPA-PET in our centre (Nîmes University Hospital, France) between November 2013 and June 2019 for

suspected primary brain tumor based on clinical and magnetic resonance imaging (MRI) findings. Inclusion criteria were presence of defined tumor (histologically confirmed) or pseudotumor (diagnosed by histological or other analyses) diagnosis, clinical and MRI follow-up of > 24 months, and FDOPA-PET scan < 2 months before surgery or stereotactic biopsy (if performed).

We screened 184 FDOPA-PET scans performed in 166 different patients with suspected primary brain tumor. In patients with several FDOPA-PET scans performed, only the initial scan was taken into account. We excluded 75 tumor patients in whom FDOPA-PET was performed after initial surgery or biopsy. In addition, 17 patients were excluded who did not conform to the inclusion criteria (i.e. no definite tumor or pseudotumor diagnosis could be made or follow-up was < 24 months), resulting in 74 patients for analysis including 26 pseudotumor and 48 tumor patients. Flowchart of patient selection is shown in Fig. 1.

Patients with a tumoral lesion were classified according to the WHO 2016 grading system into low-grade (i.e. grade I and II glioma) or high-grade (i.e. grade III and IV glioma, or other high-grade non-glioma). Genetic analyses in search for isocitrate dehydrogenase mutation and 1p/19q co-deletion were performed in grade II and III gliomas and integrated in the WHO 2016 grading system used in our study. For patients with a pseudotumoral lesion, final diagnosis was based on histology, MRI, additional blood/cerebrospinal fluid, or follow-up analyses.

### FDOPA-PET imaging and data analysis

PET-CT was performed on a GE Discovery 710 Elite system (GE Healthcare). Patients were asked to fast for at least 4 h before image acquisition. The patients were placed in supine position on the examination table, infused with a catheter, with head immobilized in a headrest. The imaging sequence started 6 min after intravenous administration of FDOPA (2 MBq/kg), with a scout view (90° angle of view, 120 kV, 30 mAs). CT scan was performed for attenuation correction (120 kV, 5mAs, pitch 0.531, slice thickness 3.75 mm, slice increment 3.27 mm, QAC filter, DFOV 25). Finally, the PET was acquired in static 3D mode for 20 min, 8 min after FDOPA injection (axial field of view 25, matrix 256 × 256). After ordered subset expectation maximization (OSEM) reconstruction using 6 iterations and 24 subsets, with attenuation, scattering and point-spread-function (PSF) correction, and 4 mm full width at half maximum (FWHM) of Gaussian filter, 47 joined axial sections of 3.26 mm were obtained.

FDOPA-PET/CT images were co-registered with MRI images, based on fluid-attenuated inversion recovery and gadolinium-enhanced T1 sequences using "Integrated Registration" software (GE Healthcare's). Using the PET-MRI fusion images, a volume of interest (VOI) was placed

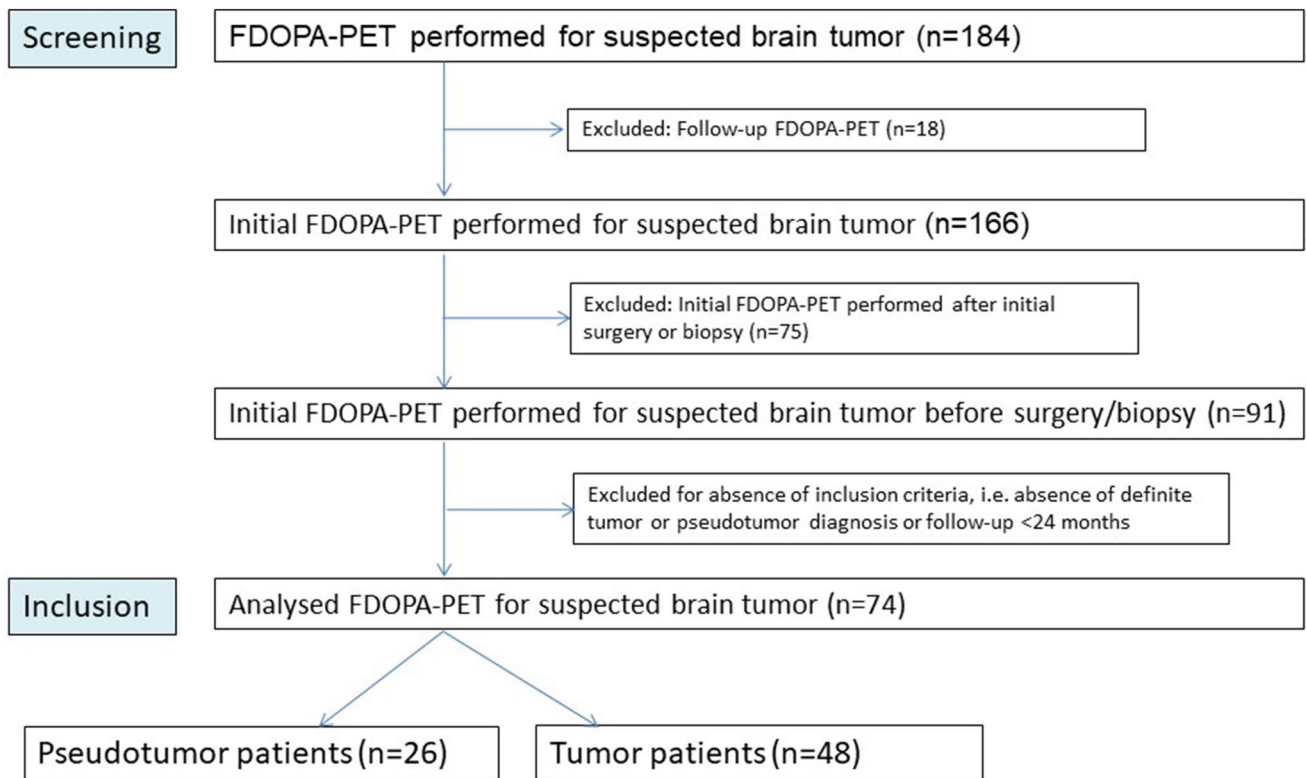


**Fig. 1** Flow chart of patient selection

directly on the lesion in case of increased FDOPA uptake by checking for congruence with the signal abnormality on the MRI corresponding to the lesion. In absence of obvious FDOPA uptake, the VOI was positioned over the MRI signal abnormality and transposed to the FDOPA-PET. For lesion F-DOPA uptake, a threshold of 42% of the maximum was used. Background reference FDOPA uptake was assessed using VOIs positioned on the contralateral basal ganglia (BG), the contralateral hemispheric grey matter (i.e. a non-spherical VOI involving the cortical area showing the most intense F-DOPA uptake on axial slices), the contralateral hemispheric white matter (i.e. a spherical VOI placed in the centrum semiovale), and the homologous mirror brain area in the contralateral hemisphere. These FDOPA-PET analyses resulted in ten quantitative parameters used in our study:  $SUV_{max}$  and  $SUV_{mean}$  of the lesion and eight lesion-to-background ratios (i.e.  $SUV_{max}$  lesion/ $SUV_{max}$  BG,  $SUV_{max}$  lesion/ $SUV_{max}$  grey matter,  $SUV_{max}$  lesion/ $SUV_{max}$  white matter,  $SUV_{max}$  lesion/ $SUV_{max}$  mirror area in contralateral hemisphere,  $SUV_{mean}$  lesion/ $SUV_{mean}$  BG,  $SUV_{mean}$  lesion/ $SUV_{mean}$  grey matter,  $SUV_{mean}$  lesion/ $SUV_{mean}$  white matter,  $SUV_{mean}$  lesion/ $SUV_{mean}$  mirror area in contralateral hemisphere).

Lesion size (maximum diameter; volume) of tumoral and pseudotumoral lesions were calculated based on the MRI,

using both gadolinium-enhancement T1-weighted imaging and FLAIR sequence (especially for lesions or part of lesions lacking gadolinium-enhancement) and by excluding signal changes corresponding to perilesional oedema, performed preceding the PET scan.

### Statistical analysis

The patients' characteristics and SUV parameters were described according to the presence of tumoral or pseudotumoral brain lesion using frequency for categorical variables and median and interquartile range (IQR) for continuous variables. The performance of the different FDOPA-PET parameters for discriminating pseudotumoral from tumoral lesions, was analysed using receiver operating curve (ROC) analysis [23]. The area under the curve (AUC) value of each SUV parameter was compared to the AUC of the other SUV parameters using the non-parametric method described by DeLong et al. [24]. We applied three cut-offs for the SUV parameters with the best AUC: (1) the cut-off that maximized the Youden's J-index (sensitivity + specificity - 1), (2) the best cut-off that maximized specificity (specificity > 95%), and the best cut-off that maximized sensitivity (sensitivity > 95%). Analyses

were performed with a bilateral alpha level of 0.05 using SAS software, version 9.4 (SAS Institute, Cary, NC, USA).

Ethics approval was obtained according to local regulations.

## Results

A total of 74 FDOPA-PET scans from 74 patients were analysed: 26 patients with pseudotumoral and 48 patients with tumoral brain lesion. Patient characteristics and

**Table 1** Patients characteristics, and lesion, background, and lesion/background SUV of the pseudotumor and tumor patients

	Non-Tumor <i>n</i> = 26	Tumor <i>n</i> = 48	Low grade Tumor <i>n</i> = 8	High grade Tumor <i>n</i> = 40
Sex				
M/F	12/14	25/23	4/4	21/19
Age				
Median; (Q1;Q3)	50.5; (38–66)	58.5; (24–84)	42.5; (37–73.5)	60; (50.5–66.5)
SUV Lesion max				
Median; (Q1;Q3)	2.09; (1.69–2.6)	1.99; (1.8–2.74)	4.11; (3.07–5.07)	3.01; (2.05–4.33)
SUV Lesion mean				
Median; (Q1;Q3)	1.33; (0.99–1.81)	1.2; (1.04–2.02)	2.34; (1.94–2.97)	1.99; (1.29–2.49)
SUV BG max				
Median; (Q1;Q3)	2.55; (2.05–2.9)	2.26; (2.15–2.77)	2.36; (2.15–2.87)	2.4; (2.12–2.87)
SUV BG mean				
Median; (Q1;Q3)	1.84; (1.53–2.21)	1.59; (1.55–1.96)	1.76; (1.44–2.06)	1.76; (1.52–2.11)
SUV GM max				
Median; (Q1;Q3)	1.72; (1.52–1.96)	1.59; (1.45–2.01)	1.71; (1.47–2.03)	1.7; (1.48–1.99)
SUV GM mean				
Median; (Q1;Q3)	1.16; (1–1.42)	1.12; (1–1.41)	1.1; (0.96–1.23)	1.12; (0.98–1.3)
SUV WM max				
Median; (Q1;Q3)	1.09; (0.91–1.29)	1.1; (0.91–1.27)	1.15; (1–1.25)	1.13; (0.97–1.25)
SUV WM mean				
Median; (Q1;Q3)	0.69; (0.63–0.84)	0.6; (0.53–0.94)	0.68; (0.56–0.79)	0.67; (0.57–0.82)
SUV Mirror area max				
Median; (Q1;Q3)	1.77; (1.43–1.96)	1.63; (1.49–2.11)	1.79; (1.61–2.2)	1.77; (1.53–2.11)
SUV Mirror area mean				
Median; (Q1;Q3)	1.04; (0.89–1.24)	1.01; (0.89–1.41)	1.09; (0.96–1.21)	1.08; (0.91–1.24)
SUV Lesion/BG max				
Median; (Q1;Q3)	0.79; (0.69–1.02)	0.86; (0.82–0.96)	1.76; (1.24–2.01)	1.12; (0.85–1.82)
SUV Lesion/BG mean				
Median; (Q1;Q3)	0.76; (0.6–0.9)	0.81; (0.67–0.97)	1.44; (1.16–1.58)	1.08; (0.76–1.5)
SUV Lesion/GM max				
Median; (Q1;Q3)	1.12; (0.97–1.51)	1.23; (1.19–1.33)	2.58; (1.97–2.95)	1.73; (1.19–2.63)
SUV Lesion/GM mean				
Median; (Q1;Q3)	1.01; (0.86–1.31)	1.08; (0.95–1.3)	2.34; (1.64–2.58)	1.62; (1.05–2.39)
SUV Lesion/WM max				
Median; (Q1;Q3)	1.84; (1.44–2.26)	2.01; (1.68–2.43)	3.53; (2.77–4.72)	2.67; (1.84–3.75)
SUV Lesion/WM mean				
Median; (Q1;Q3)	1.73; (1.6–1.98)	2.25; (1.73–2.4)	3.78; (2.8–4.41)	2.79; (1.82–4.06)
SUV Lesion/Mirror area max				
Median; (Q1;Q3)	1.21; (1.02–1.39)	1.21; (1.04–1.43)	2.29; (1.75–2.79)	1.58; (1.21–2.44)
SUV Lesion/Mirror area mean				
Median; (Q1;Q3)	1.19; (0.99–1.58)	1.26; (1.05–1.51)	2.38; (1.77–2.77)	1.72; (1.16–2.5)

*M* male, *F* female, *SUV* standardised uptake value, *SD* standard deviation, *BG* basal ganglia, *GM* grey matter, *WM* white matter

FDOPA-PET data of the different groups are shown in Table 1. Age did not differ significantly between both tumoral and pseudotumoral patients (median 58.5 vs. 50.5 years,  $p=0.16$ ).

The 48 tumor patients included 8 low-grade (grade II glioma,  $n=7$ ; grade II ependymoma,  $n=1$ ), and 40 high-grade (grade III glioma,  $n=12$ ; grade IV glioma,  $n=25$ , primary cerebral lymphoma,  $n=1$ ; medulloblastoma,  $n=1$ , and metastatic cerebral breast cancer,  $n=1$ ) tumors. Histology was available for all tumor patients.

The pseudotumor group included patients with an inflammatory lesion ( $n=11$ ), lobar primary intracerebral haemorrhage ( $n=3$ ), cortical dysplasia ( $n=3$ ), infectious lesion ( $n=2$ , both toxoplasmosis), cerebral cavernomatous malformation ( $n=1$ ), seronegative autoimmune limbic encephalitis ( $n=1$ ), deep venous sinus thrombosis-related oedema ( $n=1$ ), brain infarction ( $n=1$ ), chronic posttraumatic brain lesion ( $n=1$ ), radionecrosis after radiation therapy for arteriovenous malformation ( $n=1$ ), and mixed inflammatory/infectious lesion ( $n=1$ ). The 11 patients with an inflammatory lesion included patients with multiple sclerosis ( $n=6$ ), isolated inflammatory lesion ( $n=3$ ), solitary sclerosis ( $n=1$ ), and chronic lymphocytic inflammation with pontine perivascular enhancement responsive to steroids (CLIPPERS) ( $n=1$ ). Six pseudotumor patients had histological analysis (multiple sclerosis,  $n=2$ ; isolated inflammatory lesion,  $n=2$ ; and infectious lesion,  $n=2$ ). Demographic, diagnostic, histological, MRI and FDOPA-PET data of pseudotumoral patients are shown in Table 2.

Lesion diameter differed significantly between tumoral and pseudotumoral lesions (mean 39.3 mm vs. 27.1 mm,  $p=0.0032$ ), whereas lesion volume did not differ significantly (mean 27.8 cm<sup>3</sup> vs. 17.9 cm<sup>3</sup>,  $p=0.18$ ). Tumoral and pseudotumoral patients included no and one patient with lesion diameter < 10 mm, and two and three patients with lesion diameter < 12 mm, respectively.

Using ROC analyses, SUV<sub>max</sub> lesion/BG, SUV<sub>max</sub> lesion/grey matter, SUV<sub>mean</sub> lesion/grey matter, and SUV<sub>max</sub> lesion/mirror area in contralateral hemisphere ratios showed the highest AUC values (all AUC 0.85, 95% CI) for discriminating pseudotumoral from tumoral lesions (Fig. 2). Thresholds for optimal combined sensitivity/specificity, 95% sensitivity, and 95% specificity for SUV<sub>max</sub> lesion/BG, SUV<sub>max</sub> lesion/grey matter, SUV<sub>mean</sub> lesion/grey matter, and SUV<sub>max</sub> lesion/mirror area in contralateral hemisphere ratios are shown in Table 3.

SUV<sub>max</sub> lesion/basal ganglia ratio showed thresholds with the narrowest 95% sensitivity (SUV<sub>max</sub> lesion/basal ganglia ratio value of 0.79) and 95% specificity (SUV<sub>max</sub> lesion/basal ganglia ratio value of 1.35) window. Box-and-whisker diagrams for the SUV<sub>max</sub> lesion/basal ganglia ratio values comparing the different groups and subgroups are shown in Fig. 3. Box-and-whisker diagrams for the three

other parameters are shown in Supplemental Fig. 1. This SUV<sub>max</sub> lesion/basal ganglia 0.79–1.35 window included 16 (33%) tumor patients and 13 (50%) pseudotumor patients. Two tumor patients showed a value of < 0.79 value (i.e. 0.67 in a grade IV astrocytoma, and 0.76 in a grade II glioma) and one pseudotumor patient showed a value of > 1.35 (i.e. 2.02 in a patient with radionecrosis after radiation therapy for arteriovenous malformation). The pseudotumor patients with a SUV<sub>max</sub> lesion/basal ganglia ratio value between 1.00 (corresponding to the cut-off value often used in the literature to consider uptake as increased) and 1.35 (corresponding to the cut-off value associated with 95% specificity in our study) were: one patient with an infectious lesion (value of 1.01), three patients with an inflammatory lesion (two multiple sclerosis patients with values of 1.02 and 1.06, and one patient with an isolated inflammatory lesion with a value of 1.16), one patient with a mixed inflammatory/infectious lesion (value of 1.22), and one patient with a lobar cerebral amyloid angiopathy-related intracerebral haemorrhage (value of 1.34).

There was no statistical difference in lesion FDOPA-PET activity between pseudotumor patients with or without biopsy ( $p=0.4$  for SUV<sub>max</sub> lesion/BG).

## Discussion

SUV<sub>max</sub> lesion/BG, SUV<sub>max</sub> lesion/grey matter, SUV<sub>mean</sub> lesion/grey matter, and SUV<sub>max</sub> lesion/mirror area in contralateral hemisphere ratios were the optimal parameters to best discriminate pseudotumoral from tumoral lesions with relatively high overlap in SUV values between both groups. Optimal discriminating thresholds depended on whether sensitivity or specificity was privileged. SUV<sub>max</sub> lesion/basal ganglia showed the narrowest 95% sensitivity–95% specificity window, with one low-grade and one high-grade tumor showing SUV<sub>max</sub> lesion/basal ganglia ratio values below the value corresponding to the 95% sensitivity cut-off and one patient with radionecrosis after radiation therapy for arteriovenous malformation above the value corresponding to the 95% specificity cut off.

The patient with radionecrosis (with symptom onset related to intracranial hypertension four years after radiation therapy, and FDOPA-PET performed 2 years later) showed very high FDOPA uptake (SUV<sub>max</sub> lesion/BG ratio value of 2.02). Earlier reports analysing FDOPA-PET use for differentiating progressive brain tumor from radionecrosis (after radiation therapy for brain tumor) showed relative high sensitivity (i.e. 81% and 90%) and specificity (i.e. 84% and 92%) [19, 20, 25]. In our patient, however, radiation therapy was given for arteriovenous malformation, in the absence of brain tumor.

**Table 2** Demographic, diagnostic, histological, MRI and FDOPA-PET data of pseudotumoral patients

Patient Nr	Age	Sex	Diagnosis	Histology	MRI maximum lesion diameter (mm)	MRI lesion volume (cm <sup>3</sup> )	FDOPA-PET SUV Lesion/BG max	FDOPA-PET SUV Lesion/GM mean	FDOPA-PET SUV Lesion/Mirror area max
1	36	F	Inflammatory (Multiple sclerosis)	No	12.0	0.4	0.61	1.01	0.98
2	39	F	Inflammatory (Multiple sclerosis)	Yes	70.0	131.0	1.06	0.80	1.29
3	28	F	Inflammatory (Multiple sclerosis)	No	18.5	3.7	0.89	0.81	1.55
4	25	M	Inflammatory (Multiple sclerosis)	No	22.0	3.5	1.02	1.67	1.40
5	39	F	Inflammatory (Multiple sclerosis)	No	11.6	2.0	0.66	0.97	1.01
6	49	F	Inflammatory (Multiple sclerosis)	Yes	54.9	17.6	0.80	0.93	1.06
7	68	M	Inflammatory (Isolated inflammatory lesion)	No	12.9	2.0	0.75	0.97	1.21
8	50	F	Inflammatory (Isolated inflammatory lesion)	Yes	12.6	0.4	1.16	2.24	1.27
9	71	F	Inflammatory (Isolated inflammatory lesion)	No	17.1	3.0	0.76	1.11	1.02
10	51	M	Inflammatory (Solitary sclerosis)	No	16.7	5.3	0.73	0.92	1.07
11	64	M	Inflammatory (CLIPPERS)	No	14.0	3.3	0.59	0.84	0.98
12	83	M	Lobar primary intracerebral haemorrhage	No	66.9	170.0	0.85	1.07	1.31
13	66	F	Lobar primary intracerebral haemorrhage	No	19.0	4.3	0.69	1.05	1.29
14	60	F	Lobar primary intracerebral haemorrhage	No	24.9	4.6	1.34	1.77	1.64
15	38	F	Cortical dysplasia	No	10.3	0.2	0.66	0.70	1.01
16	18	F	Cortical dysplasia	No	13.0	1.9	0.68	0.86	0.88
17	19	F	Cortical dysplasia	No	15.0	1.6	1.14	1.56	1.68
18	33	M	Infectious (Toxoplasmosis)	Yes	6.0	0.3	0.73	0.97	1.22
19	41	M	Infectious (Toxoplasmosis)	Yes	18.6	10.6	1.01	1.31	1.34
20	75	M	Cerebral cavernomatous malformation	No	20.0	4.5	0.96	1.09	1.06
21	81	M	Autoimmune limbic encephalitis	No	22.3	3.2	0.76	1.12	1.10
22	66	F	Deep venous sinus thrombosis-related oedema	No	38.3	15.8	0.97	1.01	1.39
23	59	M	Brain infarction	No	72.1	22.9	0.36	0.65	0.90
24	59	M	Posttraumatic brain lesion	No	27.8	1.7	0.77	0.85	1.06
25	48	M	Radionecrosis	No	53.3	27.2	2.02	2.33	2.49
26	64	F	Mixed inflammatory/infectious	Yes	35.0	23.4	1.22	2.06	1.49



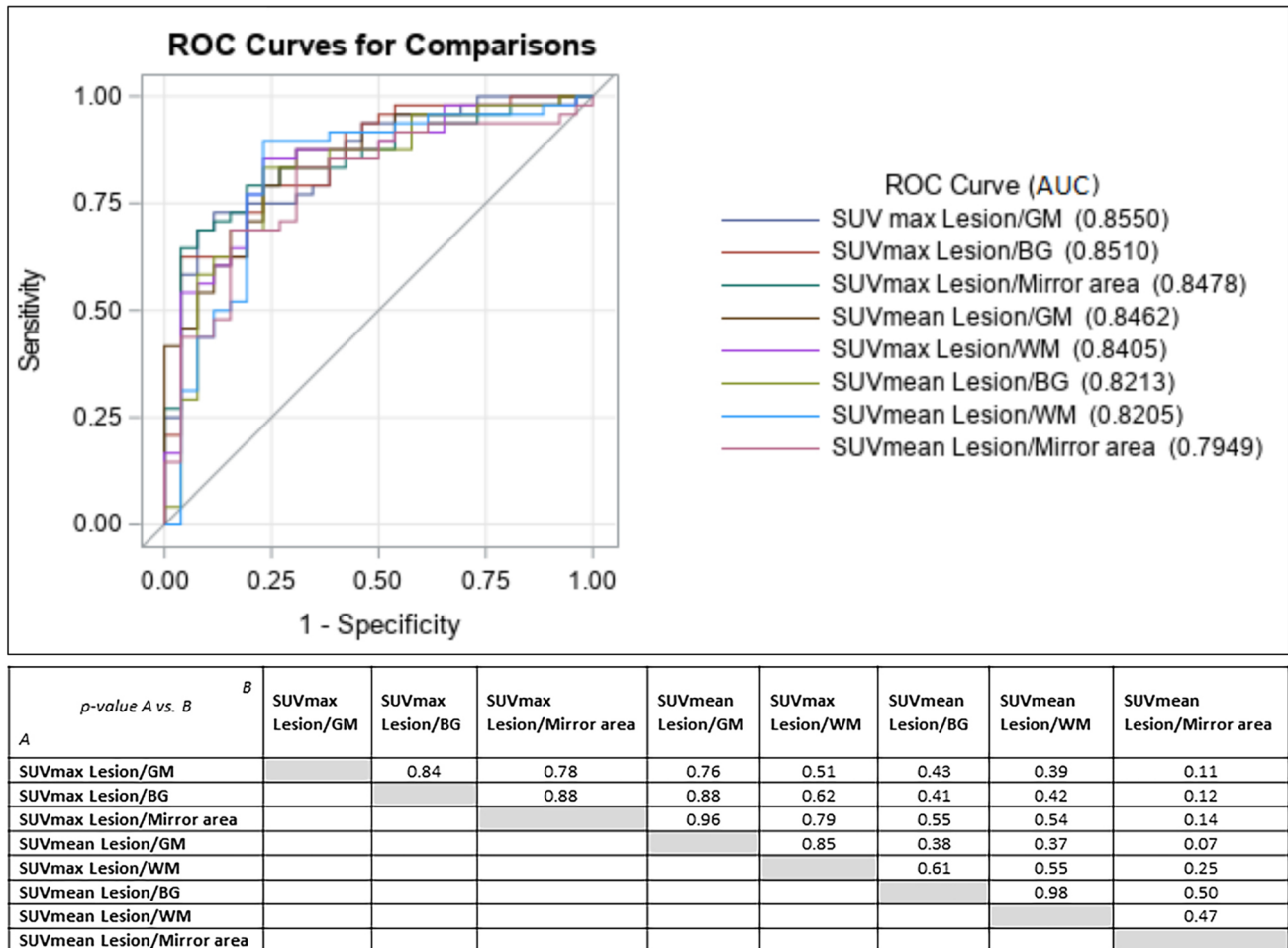


**Fig. 2** *p*-value for comparison of AUC (area under the curve) of ROC (receiver operating characteristic) curves between the different FDOPA-PET parameters A vs B. *BG* basal ganglia, *GM* grey matter, *WM* white matter

In earlier reports, different amino acid PET tracers showed high sensitivity for detecting tumoral lesions and tumor recurrence, in contrast with only moderate specificity [9, 10]. Several of these studies reporting on sensitivity and specificity of amino acid PET tracers used a threshold SUV lesion/background ratio value of 1, probably favouring sensitivity due to the relative high proportion of slightly elevated uptake in pseudotumor patients [9, 19]. The non-specific increased uptake of pseudotumoral lesions is an important issue since aggressive diagnostic and therapeutic procedures (i.e. stereotactic biopsy or surgery) may be proposed in these pseudotumoral patients based on PET data only.

Amino acid PET uptake in tumoral lesions probably reflects both tumor and vascular cells of biologically active tumor tissue together with passive tracer influx due to enhanced blood–brain barrier permeability (since tracer accumulation is associated with contrast enhancement on MRI) [8]. Therefore, enhanced blood–brain barrier permeability may play a role in the increased tracer uptake

sometimes observed in active contrast-enhancing pseudotumoral lesions. Amino acid tracer uptake has also been observed in brain areas showing reactive astrogliosis near gliomas, hematomas, infarction, inflammatory and infectious lesions [26–31]. In some of these reported lesions, increased LAT1/2 expression has been observed, probably explaining increased amino acid tracer uptake [29]. Increased LAT1/2 expression related to reactive astrogliosis may therefore also explain the increased uptake in some of these pseudotumoral, sometimes non-contrast-enhancing lesions.

In our study, all tumor patients had histology (required for inclusion), whereas less than one third of pseudotumor patients had histology, possibly creating a verification bias (i.e. PET results may have influenced the decision to biopsy or surgery) and study limitation.

Recently, reconstructed PET images using PSF correction has been shown to be non-quantitative for small lesions (< 10–12 mm), since recovery coefficients are non-monotonic as a function of lesion size, less reproducible,

**Table 3** Cut-offs for the different FDOPA-PET parameters for discriminating pseudotumor vs. tumor: cut-off for optimal combined sensitivity/specificity, for  $\geq 95\%$  specificity, and for  $\geq 95\%$  sensitivity

Variable	N	p-value*	AUC	Cut-off SUV for optimal combined sensitivity/specificity**	Sensitivity (%)	Specificity (%)	Cut-off SUV for $\geq 95\%$ specificity	Associated Sensitivity (%)	Cut-off SUV for $\geq 95\%$ sensitivity	Associated Specificity (%)
SUVmax Lesion/BG	74	0.0001	0.851	1.35	62.5	96.2	1.35	62.5	0.79	50
SUVmax Lesion/GM	74	<.0001	0.855	1.72	72.9	88.5	2.02	58.3	1.11	46.2
SUVmean Lesion/GM	74	<.0001	0.846	1.11	87.5	69.2	2.25	45.8	0.99	46.2
SUVmax Lesion/Mirror area	74	0.0002	0.848	1.67	68.8	93.2	1.78	64.6	1.02	26.9

AUC area under the curve, SUV standardised uptake value, BG basal ganglia, GM grey matter

\*p-value for Chi-square test of logistic regression

\*\*Cut-off which maximize the Youden index, i.e. (sensitivity + specificity – 1)

and more slowly converging [32]. This non-linearity may lead to a disproportionate increase of activity of small lesions [32]. Therefore, PSF correction was not recommended by the joint EANM/EANO/RANO practice guidelines/SNMMI procedure standards (published online at the end of 2018) for PET imaging of gliomas [33]. PET scans in our patients were performed between 2013 and 2019, with PSF correction in the vast majority of patients. This may have affected both tumor and reference region activity (and calculated cut-off levels) in our study patients. Therefore, cut-off levels may not be directly comparable to the values in the literature of studies using PET imaging without PSF correction. The effect of PET analysis with PSF correction in our study probably had only a minimal impact on the results since only a very small minority of patients presented with small lesions.

For FDOPA-PET, the BG is the background reference area most frequently used in the literature (and therefore also used in our study). However, since BG uptake is age dependent, uptake ratios (and the corresponding calculated cut-off values) using BG may have been impacted by the age of the included patients [34]. The age-dependant BG uptake was probably not a major study limitation since the age did not differed significantly between tumoral and pseudotumoral patients, and since similar PET results were observed when using other (i.e. than BG) reference areas in our study (although age-related uptake differences might not be excluded in those other areas neither).

## Conclusion

FDOPA-PET uptake should be interpreted with caution in patients with suspected brain tumor based on clinical and brain imaging findings, especially in patients showing low or intermediate SUV values and ratios. FDOPA-PET lesion uptake must be interpreted taking into account all clinical, radiological, and biological data to decide if other complementary analyses are needed to determine the underlying pseudotumoral cause or if aggressive diagnostic and therapeutic procedures are required in case of brain tumor. FDOPA has to be compared with other amino acid tracers to identify the PET tracer yielding optimal discriminating properties for tumoral and pseudotumoral lesions.



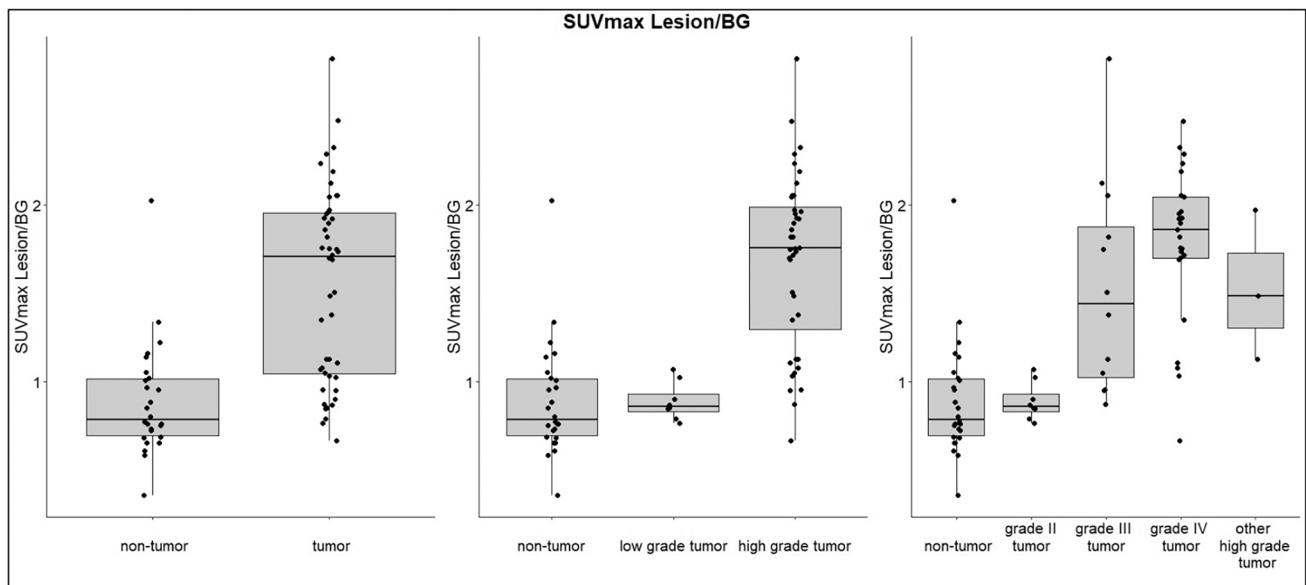


**Fig. 3** Box-and-whisker diagrams presented as medians and interquartile ranges of lesion/BG max by comparing pseudotumor vs. tumor, pseudotumor vs. low-grade tumor vs. high-grade tumor, and

pseudotumor vs. grade II glioma vs. grade III glioma vs. grade IV glioma vs. other high-grade tumor

**Acknowledgements** We would like to thank Dr. Sarah Kabani (Service de Biostatistique, Epidémiologie Clinique, Santé Publique et Innovation en Méthodologie (BESPI), CHU de Nîmes, 4 Rue du Professeur Debré, 30029 Nîmes Cedex 09) for proofreading our manuscript.

**Funding** None.

### Compliance with ethical standards

**Conflicts of interest** The authors declare that they have no conflict of interest.

**Research involving human participants and/or animals** This article does not contain any studies with animals performed by any of the authors.

**Informed consent** Informed consent was obtained from all individual participants included in the study.

### References

- Albert NL, Weller M, Suchorska B et al (2016) Response assessment in neuro-oncology working group and european association for neuro-oncology recommendations for the clinical use of PET imaging in gliomas. *Neuro Oncol* 18:1199–1208
- Filss CP, Ciccone F, Shah NJ, Galldiks N, Langen KJ (2017) Amino acid PET and MR perfusion imaging in brain tumours. *Clin Transl Imaging* 5:209–223
- Lapa C, Linsenmann T, Monoranu CM et al (2014) Comparison of the amino acid tracers 18F-FET and 18F-DOPA in high-grade glioma patients. *J Nucl Med* 55:1611–1616
- Becherer A, Karanikas G, Szabó M et al (2003) Brain tumour imaging with PET: a comparison between [18F]fluorodopa and [11C]methionine. *Eur J Nucl Med Mol Imaging* 30:1561–1567
- Kratochwil C, Combs SE, Leotta K et al (2014) Intra-individual comparison of <sup>18</sup>F-FET and <sup>18</sup>F-DOPA in PET imaging of recurrent brain tumors. *Neuro Oncol* 16:434–440
- Bund C, Heimburger C, Imperiale A et al (2017) FDOPA PET-CT of nonenhancing brain tumors. *Clin Nucl Med* 42:250–257
- Morana G, Bottoni G, Mancardi MM, Verrico A, Piccardo A (2018) Seizure-induced increased 18F-DOPA uptake in a child with diffuse astrocytoma and transient brain mri abnormalities related to status epilepticus. *Clin Nucl Med* 43:e149–e150
- Rapp M, Heinzel A, Galldiks N et al (2013) Diagnostic performance of 18F-FET PET in newly diagnosed cerebral lesions suggestive of glioma. *J Nucl Med* 54:229–235
- Hutterer M, Nowosielski M, Putzer D et al (2013) [18F]-fluoroethyl-L-tyrosine PET: a valuable diagnostic tool in neuro-oncology, but not all that glitters is glioma. *Neuro Oncol* 15:341–351
- Xiao J, Jin Y, Nie J, Chen F, Ma X (2019) Diagnostic and grading accuracy of <sup>18</sup>F-FDOPA PET and PET/CT in patients with gliomas: a systematic review and meta-analysis. *BMC Cancer* 19:767
- Giammarile F, Cinotti LE, Jouvet A et al (2004) High and low grade oligodendrogliomas (ODG): correlation of amino-acid and glucose uptakes using PET and histological classifications. *J Neurooncol* 68:263–274
- Fortin D, Cairncross GJ, Hammond RR (1999) Oligodendroglioma: an appraisal of recent data pertaining to diagnosis and treatment. *Neurosurgery* 45:1279–1291
- Ogawa T, Hatazawa J, Inugami A et al (1995) Carbon-11-methionine PET evaluation of intracerebral hematoma: distinguishing neoplastic from non-neoplastic hematoma. *J Nucl Med* 36:2175–2179
- Calabria FF, Chiaravalloti A, Jaffrain-Rea ML et al (2016) 18F-DOPA PET/CT physiological distribution and pitfalls: experience in 215 patients. *Clin Nucl Med* 41:753–760

15. Hsieh HJ, Lin SH, Chu YK, Chang CP, Wang SJ (2005) F-18 FDG and F-18 FDOPA PET brain imaging in subacute sclerosing panencephalitis. *Clin Nucl Med* 30:519–520
16. Condon L, Blazak J (2018) Focal 18F-DOPA uptake in brain parenchyma surrounding developmental venous anomalies. *Clin Nucl Med* 43:e37–e38
17. Floeth FW, Pauleit D, Sabel M et al (2006) 18F-FET PET differentiation of ring-enhancing brain lesions. *J Nucl Med* 47:776–782
18. Kebir S, Gaertner FC, Mueller M et al (2016) <sup>18</sup>F-fluoroethyl-L-tyrosine positron emission tomography for the differential diagnosis of tumefactive multiple sclerosis versus glioma: a case report. *Oncol Lett* 11:2195–2198
19. Lizarraga KJ, Allen-Auerbach M, Czernin J et al (2014) (18) F-FDOPA PET for differentiating recurrent or progressive brain metastatic tumors from late or delayed radiation injury after radiation treatment. *J Nucl Med* 55:30–36
20. Cicone F, Minniti G, Romano A et al (2015) Accuracy of F-DOPA PET and perfusion-MRI for differentiating radionecrotic from progressive brain metastases after radiosurgery. *Eur J Nucl Med Mol Imaging* 42:103–111
21. Hernández Pinzón J, Mena D, Aguilar M, Biafore F, Recondo G, Bastianello M (2016) Radionecrosis versus disease progression in brain metastasis. Value of (18)F-DOPA PET/CT/MRI. *Rev Esp Med Nucl Imagen Mol* 35:332–325
22. Sala Q, Metellus P, Taieb D, Kaphan E, Figarella-Branger D, Guedj E (2014) 18F-DOPA, a clinically available PET tracer to study brain inflammation? *Clin Nucl Med* 39:e283-285
23. Hanley JA, McNeil BJ (1982) The meaning and use of the area under a receiver operating characteristic (ROC) curve. *Radiology* 143:29–36
24. DeLong ER, DeLong DM, Clarke-Pearson DL (1988) Comparing the areas under two or more correlated receiver operating characteristic curves: a nonparametric approach. *Biometrics* 44:837–845
25. Papin-Michault C, Bonnetaud C, Dufour M et al (2016) Study of LAT1 expression in brain metastases: towards a better understanding of the results of positron emission tomography using amino acid tracers. *PLoS ONE* 11:e0157139
26. Piroth MD, Prasath J, Willuweit A et al (2013) Uptake of O-(2-[18F]fluoroethyl)-L-tyrosine in reactive astrocytosis in the vicinity of cerebral gliomas. *Nucl Med Biol* 40:795–800
27. Salber D, Stoffels G, Oros-Peusquens AM et al (2010) Comparison of O-(2-18F-fluoroethyl)-L-tyrosine and L-3H-methionine uptake in cerebral hematomas. *J Nucl Med* 51:790–797
28. Salber D, Stoffels G, Pauleit D et al (2006) Differential uptake of [18F]FET and [3H]-methionine in focal cortical ischemia. *Nucl Med Biol* 33:1029–1035
29. Hutterer M, Bumes E, Riemenschneider MJ et al (2017) AIDS-related central nervous system toxoplasmosis with increased 18F-Fluoroethyl-L-Tyrosine amino acid pet uptake due to LAT1/2 expression of inflammatory cells. *Clin Nucl Med* 4:e506–e508
30. Lohmann P, Piroth MD, Sellhaus B et al (2018) Correlation of dynamic O-(2-[<sup>18</sup>F]Fluoroethyl) L-tyrosine positron emission tomography, conventional magnetic resonance imaging, and whole-brain histopathology in a pretreated glioblastoma: a post-mortem study. *World Neurosurg* 119:e653–e660
31. Pichler R, Wurm G, Nussbaumer K, Kalev O, Silyé R, Weis S (2010) Sarcoidosis and radiation-induced astrogliosis causes pitfalls in neuro-oncologic positron emission tomography imaging by O-(2-[18F]fluoroethyl)-L-tyrosine. *J Clin Oncol* 28:e753-755
32. Munk OL, Tolbod LP, Hansen SB, Bogsrud TV (2017) Point-spread function reconstructed PET images of sub-centimeter lesions are not quantitative. *EJNMMI Phys* 4:5
33. Law I, Albert NL, Arbizu J et al (2019) Joint EANM/EANO/RANO practice guidelines/SNMMI procedure standards for imaging of gliomas using PET with radiolabelled amino acids and [(18) F]FDG: version 1.0. *Eur J Nucl Med Mol Imaging* 46:540–557
34. Kumakura Y, Vernaleken I, Buchholz HG et al (2010) Age-dependent decline of steady state dopamine storage capacity of human brain: an FDOPA PET study. *Neurobiol Aging* 31:447–463